

## Research Article

# Structural and Optical Properties of $\alpha$ -Quartz Cluster with Oxygen-Deficiency Centers

Yin Li <sup>1,2</sup>, Xi Chen <sup>1,3</sup>, Chuanghua Yang,<sup>4</sup> Liyuan Wu,<sup>1</sup> and Ru Zhang <sup>1,3</sup>

<sup>1</sup>State Key Laboratory of Information Photonics and Optical Communications, Beijing University of Posts and Telecommunications, Beijing 100876, China

<sup>2</sup>School of Science, Beijing University of Posts and Telecommunications, Beijing 100876, China

<sup>3</sup>School of Ethnic Minority Education, Beijing University of Posts and Telecommunications, Beijing 102209, China

<sup>4</sup>School of Physics and Telecommunication Engineering, Shaanxi University of Technology, Hanzhong 723001, China

Correspondence should be addressed to Ru Zhang; [optics219@163.com](mailto:optics219@163.com)

Received 27 August 2017; Accepted 26 November 2017; Published 1 April 2018

Academic Editor: Zhike Liu

Copyright © 2018 Yin Li et al. This is an open access article distributed under the Creative Commons Attribution License, which permits unrestricted use, distribution, and reproduction in any medium, provided the original work is properly cited.

The structural and optical properties of  $\alpha$ -quartz cluster with oxygen-deficiency centers (ODCs) defects have been investigated based on the density functional theory (DFT). For cluster models with ODC(I) defect, with the increasing of cluster size and shape, the equilibrium length of Si-Si bond decreases. The excitation peaks of cluster models with ODC(I) defect are from 6.87 eV to 7.39 eV, while the excitation peaks of cluster models with ODC(II) defect are from 5.20 eV to 5.47 eV. We also study the interconversion between ODCs ( $\equiv\text{Si-Si}\equiv$  bond and divalent Si) induced by UV irradiation. Our study predicted the existence of a metastable structure of ODC(I) for the first time in literature. Our results are in good agreement with the previous results and provide strong theoretical support to the viability of the processes.

## 1. Introduction

As one of the most important crystalline oxides,  $\alpha$ -quartz is widely used in microelectronics, piezoelectric devices, optical elements, and geological dating, as well as a support in heterogeneous catalysis and other fields of research and technology. Up to now, a large number of experimental and theoretical studies have been devoted to the characterization of the structure of point defects in  $\alpha$ -quartz [1–3]. Among many defect centers in  $\alpha$ -quartz, oxygen-deficiency centers (ODCs) are believed to play a vital role in the irradiation process and subsequent photostructural changes [4] and thus have attracted much attention in research [5–10].

The crystal structure and symmetry determine that at least two distinct diamagnetic ODCs can form in  $\text{SiO}_2$  and they are commonly denoted as ODC(I) and ODC(II), giving rise to the photoabsorption bands at  $\sim 7.6$  and  $\sim 5.0$  eV, respectively [4, 11]. ODC(I) is a general consensus of the “relaxed oxygen vacancy,” namely, the  $\equiv\text{Si-Si}\equiv$  bond, having

a Si-Si bond distance about 2.3 Å [4]. As for ODC(II), there has been a large amount of controversy [4, 12–14] on the structural model. At least two alternatives were proposed. One is the “unrelaxed oxygen monovacancy,” namely, the  $\equiv\text{Si}\cdots\text{Si}\equiv$  bond, having a  $\text{Si}\cdots\text{Si}$  distance similar to that of regular Si-O-Si bonding (3.1 Å) [11], and the other is the “divalent Si,” having two Si-O bonds and a lone pair of electrons in a Si  $sp^2$  hybrid orbital [15–17].

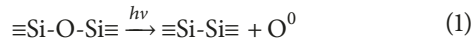
It has been found that the completely unrelaxed geometry with a Si-Si distance of 3.1 Å is not a stable arrangement and is unlikely for the ground state [17]. Indeed, the observed optical properties of ODC(II) can be reproduced almost satisfactorily by the divalent Si model rather than the unrelaxed oxygen vacancy model [18–20]. It seems that ODC(II) is more inclined to the divalent Si model. On the other hand, some researchers have shown that even a puckered unrelaxed oxygen vacancy proposed originally for  $\alpha$ -quartz has a barrier of only  $\sim 0.2$ – $0.3$  eV against the relaxation into the stable  $\equiv\text{Si-Si}\equiv$  bond [21, 22]. It was suggested that an interconversion

TABLE 1: Structural properties of the six cluster models with ODC defects in Figure 1.

Cluster size	Bond length (Å)			Bond angle (degree)	
	$d_1$	$d_2$	$d_3$	O-Si-O	Si-O-H
Si <sub>2</sub> H <sub>6</sub>	2.34	1.48	1.48	–	–
Si <sub>2</sub> O <sub>6</sub> H <sub>6</sub>	2.67	1.65	1.64	105.89	127.82
Si <sub>5</sub> O <sub>15</sub> H <sub>12</sub>	2.53	1.77	1.65	107.17	132.68
Si <sub>8</sub> O <sub>24</sub> H <sub>18</sub>	2.43	1.62	1.63	109.25	131.94
SiO <sub>2</sub> H <sub>2</sub>	1.63	1.63	0.80	100.90	–
Si <sub>3</sub> O <sub>8</sub> H <sub>6</sub>	1.67	1.64	1.62	107.70	132.19

may occur between the divalent defect and the relaxed oxygen vacancy upon ultraviolet irradiation, although a detailed mechanism of this interconversion is unknown.

In theoretical studies, it is generally accepted that the main intrinsic defect process in SiO<sub>2</sub> is the Frenkel mechanism, that is, formation of a pair of an oxygen monovacancy (Si-Si bond) and an interstitial oxygen atom (O<sup>0</sup>) from a regular Si-O-Si bond. This mechanism has been verified in amorphous SiO<sub>2</sub> [23–28], where its disordered structure influences both the defect creation and migration. Furthermore, clear experimental evidence for (1) in the ordered lattice of crystalline SiO<sub>2</sub> has been given [29]. However, the remaining main unsolved question about ODC(II) is to explain the observed close relationships between ODC(II) and ODC(I). Both centers accommodate the same amount of oxygen deficiency and it is suggested that at some configurations they can interconvert. Details of this process in  $\alpha$ -quartz are still not unambiguously established [30]



In order to reveal preferable structure of  $\alpha$ -quartz cluster with ODC(I) defect and the intrinsic mechanism of structural conversion from ODC(I) to ODC(II) in  $\alpha$ -quartz clusters, we apply the first-principles calculation to different cluster models. The size and shape effect of cluster models is included. Our study predicted the existence of a metastable structure of ODC(I) for the first time in literature. Our results also suggested the mechanism of structural conversion from ODC(I) to ODC(II) in  $\alpha$ -quartz clusters. We applied the first-principle calculation based on density functional theory (DFT) and time dependent density functional theory (TDDFT) implemented in ORCA program to the electronic structure properties and optical properties. Our paper is organized as follows. In Section 2, the models and methods are described. The results and discussions are presented in Section 3. Finally, a summary of the main conclusions of this work is given in Section 4.

## 2. Computational Methods

We have studied clusters with various size. The formulas are Si<sub>2</sub>H<sub>2</sub>, Si<sub>2</sub>O<sub>6</sub>H<sub>6</sub>, Si<sub>5</sub>O<sub>15</sub>H<sub>12</sub>, Si<sub>8</sub>O<sub>24</sub>H<sub>18</sub>, SiO<sub>2</sub>H<sub>2</sub>, and Si<sub>3</sub>O<sub>8</sub>H<sub>6</sub>, as shown in Figure 1.

In order to avoid the spurious states caused by the –O• defects located the boundary of the cluster, we use hydrogen atoms to passivate all clusters. The distance between the

capping hydrogen atoms and the oxygen atoms is 0.80 Å [31]. In the process of optimization, the interior atoms were allowed to move freely, while the terminal hydrogen atoms and surface oxygen atoms were frozen. The main geometrical parameters are given for each cluster in Table 1.

The ORCA quantum chemistry program was used in all calculations. DFT and the hybrid density functional B3LYP method [32, 33] were employed to perform the geometry optimization. Following geometry optimization, TDDFT (nroots = 16) was used for the sake of calculating the electronic excited states. Triple- $\zeta$ -quality basis sets with one set of polarization functions (TZVP) were employed for the Si, O, and H atoms, respectively [34]. In the self-consistent field calculations, tight scf convergence and a dense integration grid were selected. The maximum element of the direct inversion of iterative subspaces (DIIS) error vector is set as  $5 \times 10^{-7}$ . The structural optimization is allowed to be relaxed until the maximum force on each atom becomes less than 0.01 eV/Å and maximum energy change between two steps is smaller than  $1 \times 10^{-8}$  Eh. The density change is no more than  $1 \times 10^{-7}$  Eh [35, 36].

## 3. Results and Discussion

*3.1. Preferable Structure of  $\alpha$ -Quartz Cluster with ODC(I) Defect.* ODC(I) defect pair is created by shifting an interstitial oxygen atom (O<sup>0</sup>) from a regular Si-O-Si bond and constitutes a pair of an oxygen monovacancy (Si-Si bond) (see (1)). In (1), bonds with three oxygen atoms were represented by  $\equiv$ . For the purpose of finding out the cluster models which have the stable structure, prediction of the apposite Si-Si band length becomes a key object. The Si-Si band length ( $d_1$ ) increased from 2.0 Å to 3.5 Å, which is the main structure change, as shown in Figures 1(a)–1(d). Figure 2 shows the relationship between the total energy and Si-Si bond length in singlet state of four clusters with ODC(I) defects. The total energy of the  $\alpha$ -quartz clusters will have the lowest value along with the increasing of the Si-Si bond length. The cluster size can represent a bulk structure. In order to describe the singlet state adequately, relaxation processes were performed with four cluster models.

To improve the accuracy of the calculations, we consider the parent molecule disilane, Si<sub>2</sub>H<sub>6</sub> cluster model (see Figure 1(a)). The cluster model contains a direct Si-Si bond. As a result of the structural scan and geometry optimization, we have found that, in Figure 2(a), the equilibrium bond length in singlet state of Si<sub>2</sub>H<sub>6</sub> cluster model is 2.34 Å, similar to

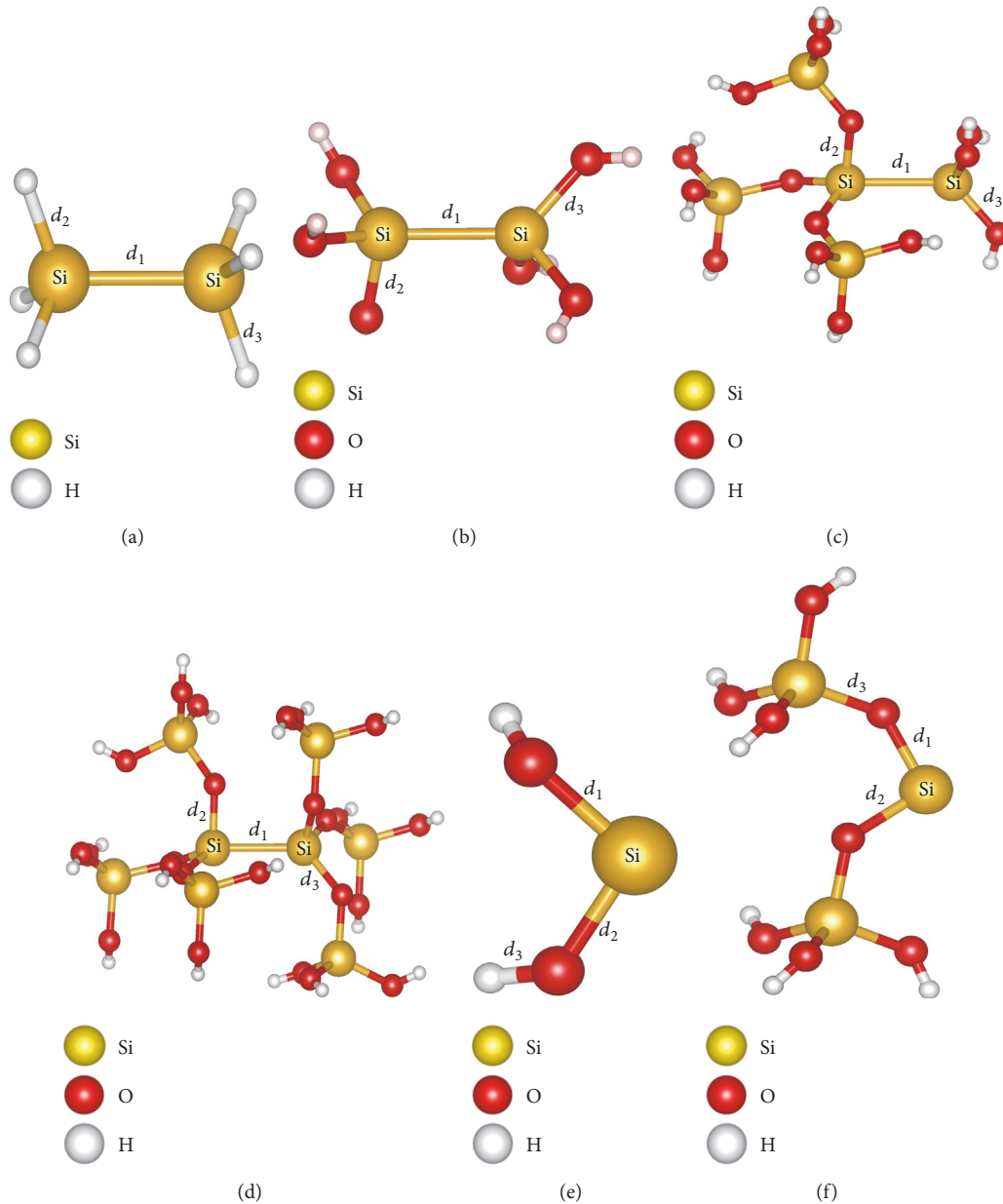


FIGURE 1: Illustrations of each of the six clusters used for  $S_0 \rightarrow S_1$  transition energy for  $\alpha$ -quartz cluster configurations with oxygen-deficiency centers. (a)  $\text{Si}_2\text{H}_6$  with ODC(I), (b)  $\text{Si}_2\text{O}_6\text{H}_6$  with ODC(I), (c)  $\text{Si}_5\text{O}_{15}\text{H}_{12}$  with ODC(I), (d)  $\text{Si}_8\text{O}_{24}\text{H}_{18}$  with ODC(I), (e)  $\text{SiO}_2\text{H}_2$  with ODC(II), and (f)  $\text{Si}_3\text{O}_8\text{H}_6$  with ODC(II). We use hydrogen atoms to passivate the oxygen atoms which terminate our cluster models.

the ordinary Si-Si bond length of 2.36 Å [31]. However, Figures 2(b)–2(d) show that the singlet state equilibrium bond lengths of  $\text{Si}_2\text{O}_6\text{H}_6$ ,  $\text{Si}_5\text{O}_{15}\text{H}_{12}$ , and  $\text{Si}_8\text{O}_{24}\text{H}_{18}$  cluster models are 2.67 Å, 2.53 Å, and 2.43 Å. With the increasing of cluster size and shape, the equilibrium Si-Si bond length decreases.

**3.2. Electronic Structure Properties and Optical Properties of ODC(I).** We compared the electronic density of states (DOS) of the four clusters with ODC(I) defects (see Figure 1) so that the geometric effect on the electronic structure can be seen clearly. Figure 3 shows the total electronic DOS for  $\text{Si}_2\text{H}_6$ ,  $\text{Si}_2\text{O}_6\text{H}_6$ ,  $\text{Si}_5\text{O}_{15}\text{H}_{12}$ , and  $\text{Si}_8\text{O}_{24}\text{H}_{18}$  clusters. In a nutshell,

the electronic DOS of all the clusters shows notable structural sensitivity. The DOS for  $\text{Si}_2\text{H}_6$  cluster reveals more uniform distributions than the other three cases, because of the small size. When the valence band states participate in optical transitions of point defects, the structural dependence of electronic state will result in different OA spectra.

The wave function of highest occupied molecular orbital (HOMO) and the electron localization function (ELF) are used to analyze the electronic structure of cluster with ODC(I) defect. We calculate the ELF and the wave function of HOMO on four clusters (see Figures 1(a)–1(d)) to clarify the charge distribution around ODC(I) defect. From the electron

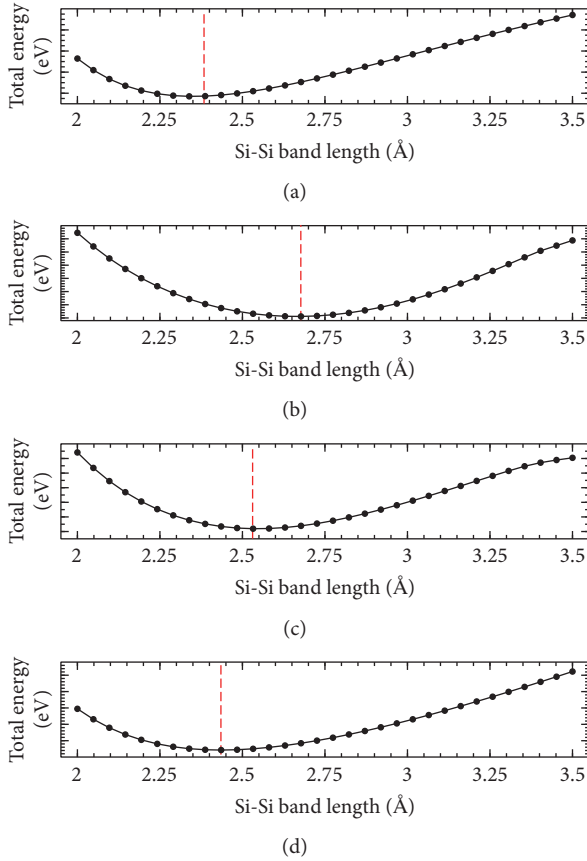


FIGURE 2: The relationship between total energy and Si-Si bond length in the four clusters with ODC(I) defects. (a)  $\text{Si}_2\text{H}_6$ , (b)  $\text{Si}_2\text{O}_6\text{H}_6$ , (c)  $\text{Si}_5\text{O}_{15}\text{H}_{12}$ , and (d)  $\text{Si}_8\text{O}_{24}\text{H}_{18}$ .

density, we can approximately derive ELF, introduced by Becke and Edgecombe [37]. The ELF pictures are shown in Figure 4. For the singlet state of the clusters, the ELF was, respectively, computed using the DFT/B3LYP, at the stable geometry of the singlet state. The nature of bonding between Si-Si atoms and charge transfer process is shown in the ELF. The transition can be depicted as an excitation from the top valence band to the ODC(I) defect level in the gap. The excited electron of the ODC(I) defect is located mainly on the central silicon atom. Figures 4(e)–4(h) show the wave function of HOMO. The excited electron transfer in the ODC(I) defect can be found in here too.

Table 2 and Figure 5 show the optical properties calculated from four clusters with ODC(I) defects by TDDFT-B3LYP, neglecting other paramagnetic defects. The singlet-to-singlet ( $s_0 \rightarrow s_1$ ) excitation energy of  $\text{Si}_2\text{H}_6$  cluster was calculated to be 7.39 eV, which agrees well with the previously reported excitation energies ( $\sim 7.6$  eV) [36, 38]. On the other hand, the calculated  $s_0 \rightarrow s_1$  excitation energy of  $\text{Si}_2\text{O}_6\text{H}_6$ ,  $\text{Si}_5\text{O}_{15}\text{H}_{12}$ , and  $\text{Si}_8\text{O}_{24}\text{H}_{18}$  clusters was 6.87–7.04 eV. These excitation energy values are only slightly smaller than the experimental  $s_0 \rightarrow s_1$  transition energy ( $\sim 7.6$  eV), because the basis sets (def2-TZVP) may not be flexible for highly energy. Analyzing these data, the nature of the 7.6 eV absorption band

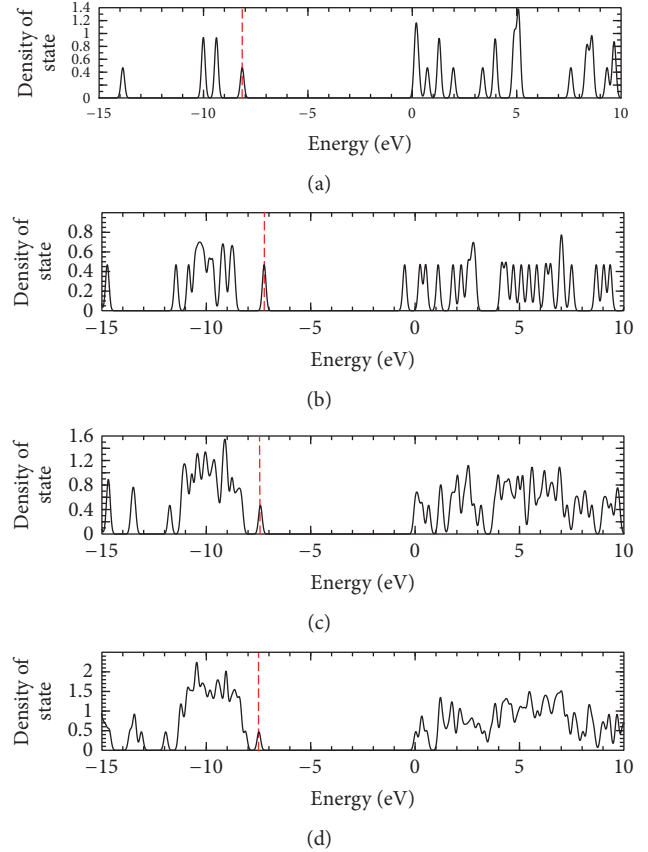


FIGURE 3: Total density of states (TDOS) of four clusters with ODC(I) defect. (a)  $\text{Si}_2\text{H}_6$ , (b)  $\text{Si}_2\text{O}_6\text{H}_6$ , (c)  $\text{Si}_5\text{O}_{15}\text{H}_{12}$ , and (d)  $\text{Si}_8\text{O}_{24}\text{H}_{18}$ . The red vertical dashed lines align to highlight highest occupied molecular orbital (HOMO) level.

cannot be ascribed to a single point defect in  $\alpha$ -quartz with ODC(I) defects. It can be explained as a manifestation of the localized states of the disordered structure of silica modified by an oxygen deficit.

**3.3. Electronic Structure Properties and Optical Properties of ODC(II).** The ODC(II) defect has been the subject of considerable interest since the discovery of the photorefractive effect in  $\text{SiO}_2$ , and consequently, their microscopic structure and optical properties have been extensively studied using the cluster approach. Figure 6 shows the DOS of the  $\alpha$ -quartz cluster models with ODC(II) defects computed by DFT-B3LYP. We calculate the total electronic DOS for  $\text{SiO}_2\text{H}_2$  and  $\text{Si}_3\text{O}_8\text{H}_6$  clusters (see Figures 1(e) and 1(f)), so that we can explore the geometric effect on the electronic structure. On the whole, the electronic DOS of the cluster shows remarkable structural sensitivity. We note that the details of the electronic structure are essentially dependent on the  $\alpha$ -quartz cluster size and shape. Such structural dependence of electronic state will result in different excitation energy when these valence band states participate in optical transition of point defects.

To further illustrate the electronic structure of cluster with ODC(II) defect, we also present the electron localization

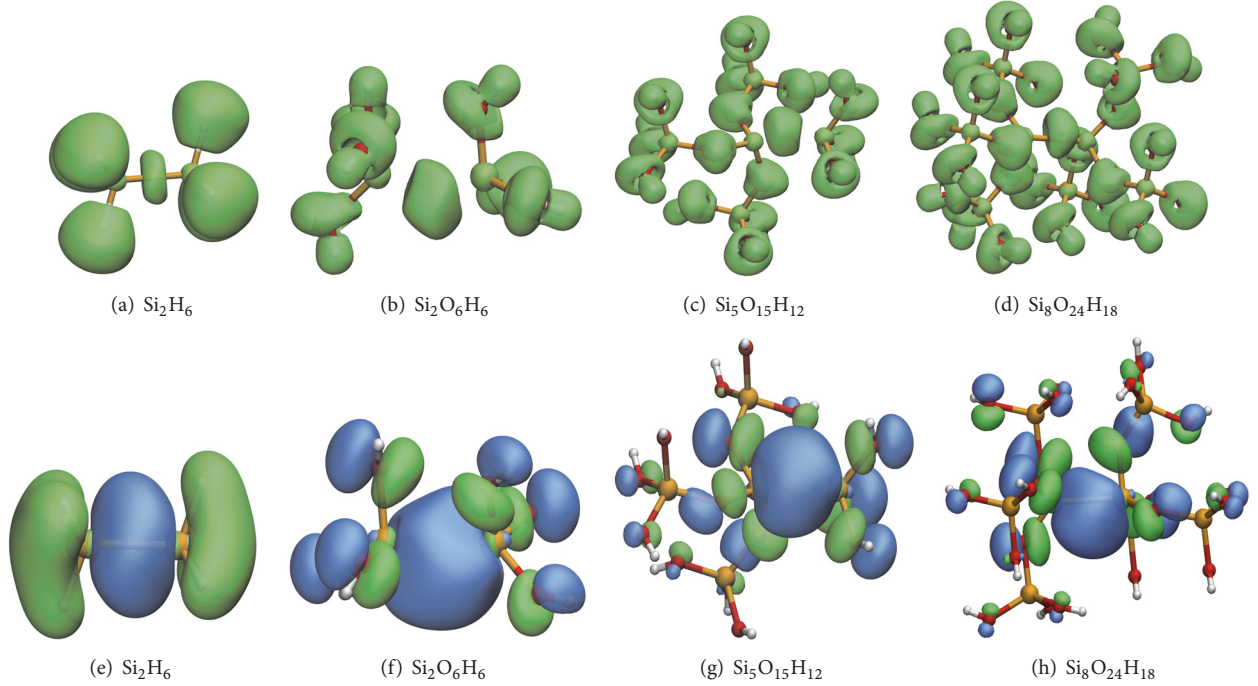


FIGURE 4: (a)–(d) ELF of the Si-Si band in  $\alpha$ -quartz cluster configurations with ODC(I); (e)–(h) orbital wave function of HOMO in  $\alpha$ -quartz cluster configurations with ODC(I). Green and blue color represent positive and negative phase of the orbital wave function, respectively.

TABLE 2: Summary of computed  $s_0 \rightarrow s_1$  transition energy of the cluster configurations with ODC(I) defects, neglecting other paramagnetic defects.

Cluster size	Transition energy (eV)	Oscillator strength $f$	Reference value (eV)
Si <sub>2</sub> H <sub>6</sub>	7.39	0.03	8.66 <sup>a</sup>
Si <sub>2</sub> O <sub>6</sub> H <sub>6</sub>	6.87	0.44	7.47 <sup>a</sup>
Si <sub>5</sub> O <sub>15</sub> H <sub>12</sub>	7.04	0.15	7.60 <sup>b</sup>
Si <sub>8</sub> O <sub>24</sub> H <sub>18</sub>	6.88	0.09	

<sup>a</sup>Reference [27]. <sup>b</sup>Reference [29].

function (ELF) (see Figures 7(a) and 7(b)) and the wave function (see Figures 7(c) and 7(d)) of HOMO on the two clusters. In order to research the charge distribution around ODC(II) defect, we plotted the ELF. For the singlet state of the clusters, the ELF was, respectively, computed using the DFT/B3LYP. The nature of divalent Si and charge transition process can be obtained in the ELF picture. The transition can be described as the lowest singlet excited state corresponding to a single electron promotion from the Si lone pair  $sp$  orbital to a vacant  $p_\pi$  orbital on the same atom. The excited electron of the ODC(II) defect is located mainly on the central silicon atom. The wave function of HOMO is shown in Figures 7(c) and 7(d). The excited electron transfer in the ODC(II) defect can also be found.

Table 3 shows the optical properties calculated from two clusters with ODC(II) defects by TDDFT-B3LYP, neglecting other paramagnetic defects.  $s_0 \rightarrow s_1$  transition energies of the SiO<sub>2</sub> with ODC(II) defects were calculated by Trukhin [10], Lü et al. [8], and Adelstein et al. [7] using different cluster models and different levels of theory. These studies yield

almost the same calculated results concerning  $s_0 \rightarrow s_1$ . In our work, the  $s_0 \rightarrow s_1$  transition energies of Si<sub>2</sub>H<sub>6</sub> and Si<sub>3</sub>O<sub>8</sub>H<sub>6</sub> clusters are, respectively, calculated to be 5.47 eV and 5.20 eV, which agree well with the previously reported excitation energies. Analyzing these data, the nature of the 5.0 eV absorption band can be ascribed to a single electron promotion from the Si lone pair  $sp$  orbital to a vacant  $p_\pi$  orbital on the same atom.

**3.4. Photoinduced Interconversions of ODC Defects in  $\alpha$ -Quartz.** A theoretical study of the interconversion models of amorphous silicon dioxide has been performed by Uchino et al. [39] who proposed a mechanism for the ODC(I)  $\rightarrow$  ODC(II) transformation based on photoionization of ODC(I). However, a detailed mechanism of this interconversion in  $\alpha$ -quartz is unknown. To get better knowledge about the detailed photoinduced interconversion mechanism of ODC defects in  $\alpha$ -quartz, we here employ quantum-chemical program (ORCA) using Si<sub>5</sub>O<sub>15</sub>H<sub>12</sub> cluster model.

Starting from the ground state geometry of Si<sub>5</sub>O<sub>15</sub>H<sub>12</sub> cluster model with ODC(I) (see Figure 1(c)), we have excited

TABLE 3: Summary of computed  $s_0 \rightarrow s_1$  transition energy for the ODC(II) defects cluster configurations, neglecting other paramagnetic defects.

Cluster size	Transition energy (eV)	Oscillator strength $f$	Reference value (eV)	Experiment (eV)
$\text{Si}_2\text{H}_6$	5.47	0.17	5.50 <sup>a</sup> , 5.60 <sup>b</sup>	5.0 <sup>d</sup>
$\text{Si}_3\text{O}_8\text{H}_6$	5.20	0.14	5.17 <sup>c</sup> , 5.30 <sup>b</sup>	

<sup>a</sup>Reference [24]. <sup>b</sup>References [8, 28]. <sup>c</sup>Reference[27]. <sup>d</sup>Reference [6].

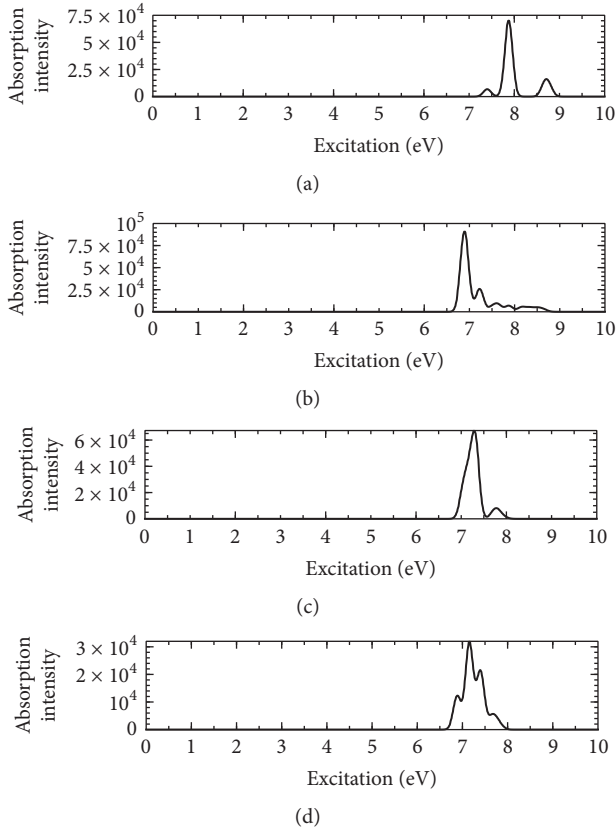


FIGURE 5: The OA spectra of four clusters calculated by TDDFT, which have ODC(I) defects. Gaussian broadening of 0.5 eV is used. (a)  $\text{Si}_2\text{H}_6$ , (b)  $\text{Si}_2\text{O}_6\text{H}_6$ , (c)  $\text{Si}_5\text{O}_{15}\text{H}_{12}$ , and (d)  $\text{Si}_8\text{O}_{24}\text{H}_{18}$ .

the model into the triplet ( $T_1$ ) state which is 4.11 eV higher in single point energy [31]. The cluster model relaxes under the modified potential energy surface, the Si-Si disconnects and expands up to 3.02 Å (see Figure 8(a)), which is slightly longer than the equilibrium bond length (2.53 Å) calculated for Figure 1(c), thus inducing a large distortion surrounding the defect. Following the reaction path toward the ODC(II) (see Figure 8(c)), we find the transition state (see Figure 8(b)) and the computed relaxation energy is 0.46 eV higher than the  $T_1$  state of  $\text{Si}_5\text{O}_{15}\text{H}_{12}$  cluster model with ODC(I). The transition state cannot be stable.

By further decreasing the reaction coordinate,  $\text{Si}_5\text{O}_{15}\text{H}_{12}$  cluster transforms spontaneously into the ODC(II) configuration and the computed relaxation energy is 0.30 eV lower than the transition state of  $\text{Si}_5\text{O}_{15}\text{H}_{12}$  cluster model. This implies that the transition state configuration corresponds to

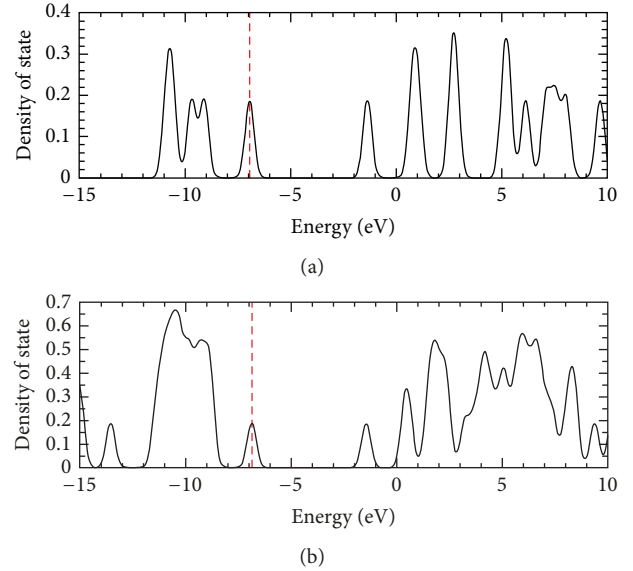


FIGURE 6: Total density of states (TDOS) of two clusters with ODC(II) defect. (a)  $\text{SiO}_2\text{H}_2$ ; (b)  $\text{Si}_3\text{O}_8\text{H}_6$ . The red vertical dashed lines align to highlight highest occupied molecular orbital (HOMO) level.

a metastable minimum and is possible to relax into a lower energy configuration shown in Figure 8(c) during thermal processes. Among the many possible local configurations of the ODC(I) defect in  $\alpha$ -quartz, only a small fraction is expected to transform into the ODC(II) upon excitation. Although our used cluster model is small, other local configurations different from ours may be more favorable for the interconversion.

## 4. Conclusions

The DFT method was employed to study the structures of six different cluster models for  $\alpha$ -quartz with ODCs defects. We predict the apposite Si-Si band length in order to search for the stable structure of cluster models with ODC(I) defects. For  $\text{Si}_2\text{O}_6\text{H}_6$ ,  $\text{Si}_5\text{O}_{15}\text{H}_{12}$ , and  $\text{Si}_8\text{O}_{24}\text{H}_{18}$  cluster models with ODC(I) defect, with the increasing of cluster size and shape, the equilibrium Si-Si bond length decreases. The OA spectroscopic properties and excitation energies are calculated based on TDDFT. For clusters with ODC(I), the nature of the 7.6 eV absorption band can be explained as a manifestation of the localized states of the disordered structure of silica modified by an oxygen deficit. However, for clusters with ODC(II), the nature of the 5.0 eV absorption band can be

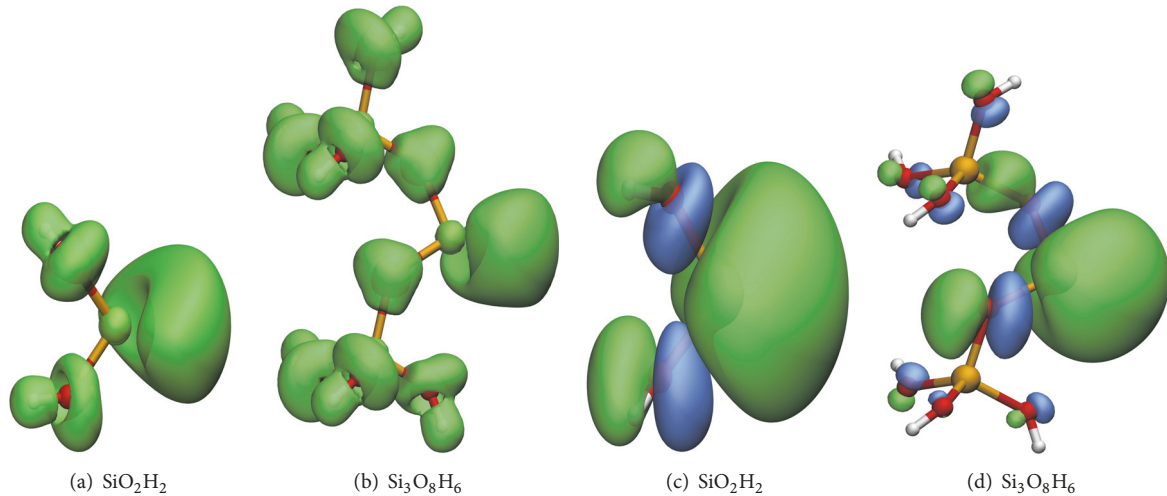


FIGURE 7: (a)-(b) ELF of the divalent Si in  $\alpha$ -quartz cluster configurations with ODC(II). (c)-(d) Orbital wave function of HOMO in  $\alpha$ -quartz cluster configurations with ODC(II). Green and blue color represent positive and negative phase of the orbital wave function, respectively.

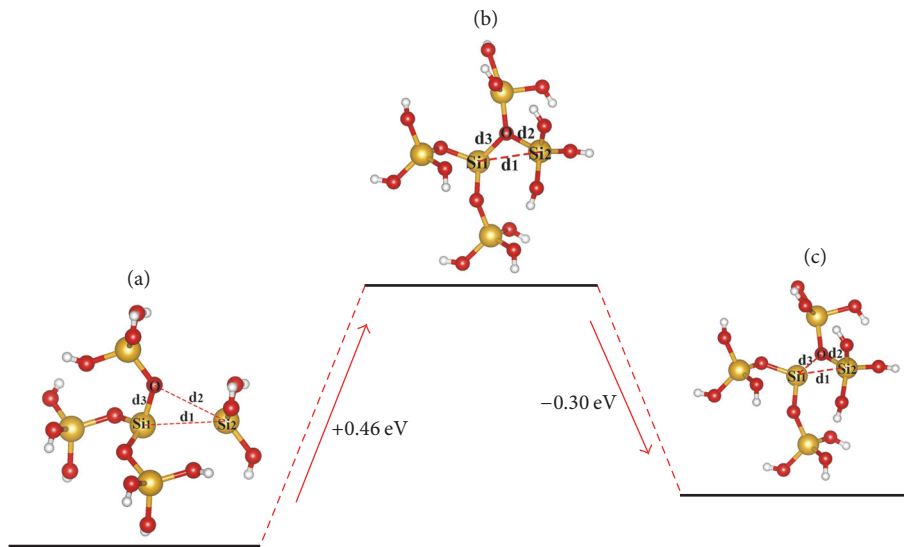


FIGURE 8: Schematic illustration of the proposed interconversion mechanism from ODC(I) defect into ODC(II) defect in the lowest triplet ( $T_1$ ) excited state. The red arrows stand for transformation of preexisting point defects and recombinations. (a) Optimized geometry of the  $\text{Si}_5\text{O}_{15}\text{H}_{12}$  cluster with ODC(I),  $d_1 = 3.02 \text{ \AA}$ ,  $d_2 = 3.05 \text{ \AA}$ , and  $d_3 = 1.65 \text{ \AA}$ . (b) The transition state geometry of the  $\text{Si}_5\text{O}_{15}\text{H}_{12}$  cluster,  $d_1 = 3.13 \text{ \AA}$ ,  $d_2 = 1.86 \text{ \AA}$ , and  $d_3 = 1.80 \text{ \AA}$ . (c) Optimized geometry of the  $\text{Si}_5\text{O}_{15}\text{H}_{12}$  cluster with ODC(II),  $d_1 = 3.07 \text{ \AA}$ ,  $d_2 = 1.64 \text{ \AA}$ , and  $d_3 = 1.91 \text{ \AA}$ .

ascribed to a single electron promotion from the Si lone pair  $sp$  orbital to a vacant  $p_\pi$  orbital on the same atom. We also study the detailed photoinduced interconversion mechanism of ODCs defects in  $\alpha$ -quartz. We predicted the existence of a metastable structure of ODC(I) for the first time. Our results provide strong theoretical support to the viability of the processes.

### Conflicts of Interest

There are no conflicts of interest related to this paper.

### Acknowledgments

This work is supported by the National Natural Science Foundation of China (nos. 61377097, 61675032, and 61671085), the National Basic Research Program of China (973 Program) under Grant no. 2014CB643900, the Open Program of State Key Laboratory of Functional Materials for Informatics, National Natural Science Foundation for Theoretical Physics Special Fund "Cooperation Program" (no. 11547039), Shaanxi Institute of Scientific Research Plan Projects (no. SLGKYQD2-05), and the Fund of State Key Laboratory

of Information Photonics and Optical Communications (BUPT) (no. IPOC2015ZT05). The authors acknowledge the computational support from the Beijing Computational Science Research Center (CSRC).

## References

- [1] A. N. Trukhin, K. Smits, J. Jansons, and A. Kuzmin, "Luminescence of polymorphous SiO<sub>2</sub>," *Radiation Measurements*, 2015.
- [2] S. Basu, "Defect related luminescence in silicon dioxide network: a review," *Crystalline Silicon-Properties and Uses: InTech*, 2011.
- [3] M. Liu, P.-F. Lu, Y. Yang, L.-Y. Wu, R. Su, and J. Chen, "Structural and Optical Properties of Point Defects in  $\alpha$ -SiO<sub>2</sub> Cluster," *Communications in Theoretical Physics*, vol. 64, no. 2, pp. 244–248, 2015.
- [4] L. Skuja, "Optically active oxygen-deficiency-related centers in amorphous silicon dioxide," *Journal of Non-Crystalline Solids*, vol. 239, no. 1–3, pp. 16–48, 1998.
- [5] R. Saavedra, D. Jiménez-Rey, P. Martin, and R. Vila, "Ionoluminescence of fused silica under swift ion irradiation," *Nuclear Instruments and Methods in Physics Research Section B: Beam Interactions with Materials and Atoms*, vol. 382, pp. 96–100, 2016.
- [6] A. N. Trukhin, "Radiation processes in oxygen-deficient silica glasses: Is ODC(I) a precursor of E1-center?" *Journal of Non-Crystalline Solids*, vol. 352, no. 28–29, pp. 3002–3008, 2006.
- [7] N. Adelstein, D. Lee, J. L. DuBois, and V. Lordi, *Magnetic fluctuation from oxygen deficiency centers on the SiO<sub>2</sub> surface*, 2014, <https://arxiv.org/abs/1403.0685>.
- [8] H.-B. Lü, S.-Z. Xu, H.-J. Wang, X.-D. Yuan, C. Zhao, and Y. Q. Fu, "Evolution of oxygen deficiency center on fused silica surface irradiated by ultraviolet laser and posttreatment," *Advances in Condensed Matter Physics*, vol. 2014, Article ID 769059, 2014.
- [9] M. L. Crespillo, J. T. Graham, Y. Zhang, and W. J. Weber, "In-situ luminescence monitoring of ion-induced damage evolution in SiO<sub>2</sub> and Al<sub>2</sub>O<sub>3</sub>," *Journal of Luminescence*, vol. 172, pp. 208–218, 2016.
- [10] A. N. Trukhin, "Luminescence of localized states in silicon dioxide glass. A short review," *Journal of Non-Crystalline Solids*, vol. 357, no. 8–9, pp. 1931–1940, 2011.
- [11] H. Imai, K. Arai, H. Imagawa, H. Hosono, and Y. Abe, "Two types of oxygen-deficient centers in synthetic silica glass," *Physical Review B: Condensed Matter and Materials Physics*, vol. 38, no. 17, pp. 12772–12775, 1988.
- [12] N. L. Anderson, R. P. Vedula, P. A. Schultz, R. M. Van Ginhoven, and A. Strachan, "First-principles investigation of low energy E1 center precursors in amorphous silica," *Physical Review Letters*, vol. 106, no. 20, Article ID 206402, 2011.
- [13] N. L. Anderson, R. Pramod Vedula, P. A. Schultz, R. M. V. Ginhoven, and A. Strachan, "Defect level distributions and atomic relaxations induced by charge trapping in amorphous silica," *Applied Physics Letters*, vol. 100, no. 17, Article ID 172908, 2012.
- [14] D. L. Griscom, "Trapped-electron centers in pure and doped glassy silica: A review and synthesis," *Journal of Non-Crystalline Solids*, vol. 357, no. 8–9, pp. 1945–1962, 2011.
- [15] K. Awazu, H. Kawazoe, and K.-I. Muta, "Optical properties of oxygen-deficient centers in silica glasses fabricated in H<sub>2</sub> or vacuum ambient," *Journal of Applied Physics*, vol. 70, no. 1, pp. 69–74, 1991.
- [16] A. R. Silin and L. N. Skuja, "Intrinsic defects in fused silica," *Journal of Non-Crystalline Solids*, vol. 71, no. 1–3, pp. 443–445, 1985.
- [17] L. Skuja, "Isoelectronic series of twofold coordinated Si, Ge, and Sn atoms in glassy SiO<sub>2</sub>: a luminescence study," *Journal of Non-Crystalline Solids*, vol. 149, no. 1–2, pp. 77–95, 1992.
- [18] G. Pacchioni and R. Ferrario, "Optical transitions and EPR properties of two-coordinated Si, Ge, Sn and related H(I), H(II), and H(III) centers in pure and doped silica from ab initio calculations," *Physical Review B: Condensed Matter and Materials Physics*, vol. 58, no. 10, pp. 6090–6096, 1998.
- [19] B. B. Stefanov and K. Raghavachari, "Cluster models for the photoabsorption of divalent defects in silicate glasses: Basis set and cluster size dependence," *Applied Physics Letters*, vol. 71, no. 6, pp. 770–772, 1997.
- [20] B. L. Zhang and K. Raghavachari, "Photoabsorption and photoluminescence of divalent defects in silicate and germanosilicate glasses: First-principles calculations," *Physical Review B: Condensed Matter and Materials Physics*, vol. 55, no. 24, pp. R15993–R15996, 1997.
- [21] M. Boero, A. Pasquarello, J. Sarnthein, and R. Car, "Structure and hyperfine parameters of E1 centers in  $\alpha$ -quartz and in vitreous SiO<sub>2</sub>," *Physical Review Letters*, vol. 78, no. 5, pp. 887–890, 1997.
- [22] K. C. Snyder and W. B. Fowler, "Oxygen vacancy in  $\alpha$ -quartz: A possible bi- and metastable defect," *Physical Review B: Condensed Matter and Materials Physics*, vol. 48, no. 18, pp. 13238–13243, 1993.
- [23] H. Hosono, H. Kawazoe, and N. Matsunami, "Experimental evidence for frenkel defect formation in amorphous SiO<sub>2</sub> by electronic excitation," *Physical Review Letters*, vol. 80, no. 2, pp. 317–320, 1998.
- [24] K. Kajihara, M. Hirano, L. Skuja, and H. Hosono, "Formation of intrinsic point defects in fluorine-doped synthetic SiO<sub>2</sub> glass by <sup>60</sup>Co  $\gamma$ -ray irradiation," *Chemistry Letters*, vol. 36, no. 2, pp. 266–267, 2007.
- [25] K. Kajihara, M. Hirano, L. Skuja, and H. Hosono, "Intrinsic defect formation in amorphous SiO<sub>2</sub> by electronic excitation: Bond dissociation versus Frenkel mechanisms," *Physical Review B: Condensed Matter and Materials Physics*, vol. 78, no. 9, Article ID 094201, 2008.
- [26] L. Skuja, B. Güttler, D. Schiel, and A. R. Silin, "Infrared photoluminescence of preexisting or irradiation-induced interstitial oxygen molecules in glassy SiO<sub>2</sub> and  $\alpha$ -quartz," *Physical Review B: Condensed Matter and Materials Physics*, vol. 58, no. 21, pp. 14296–14304, 1998.
- [27] M. A. Stevens-Kalceff, "Electron-Irradiation-Induced Radiolytic Oxygen Generation and Microsegregation in Silicon Dioxide Polymorphs," *Physical Review Letters*, vol. 84, no. 14, pp. 3137–3140, 2000.
- [28] T. E. Tsai and D. L. Griscom, "Experimental evidence for excitonic mechanism of defect generation in high-purity silica," *Physical Review Letters*, vol. 67, no. 18, pp. 2517–2520, 1991.
- [29] K. Kajihara, L. Skuja, and H. Hosono, "Formation and annihilation of intrinsic defects induced by electronic excitation in high-purity crystalline SiO<sub>2</sub>," *Journal of Applied Physics*, vol. 113, no. 14, Article ID 143511, 2013.
- [30] G. Pacchioni and G. Ieraño, *Physical Review B: Condensed Matter and Materials Physics*, vol. 57, no. 2, pp. 818–832, 1998.
- [31] B. B. Stefanov and K. Raghavachari, "Photoabsorption of the neutral oxygen vacancy in silicate and germanosilicate glasses:

- First-principles calculations,” *Physical Review B: Condensed Matter and Materials Physics*, vol. 56, no. 9, pp. 5035–5038, 1997.
- [32] A. D. Becke, “Density-functional thermochemistry. III. The role of exact exchange,” *The Journal of Chemical Physics*, vol. 98, no. 7, pp. 5648–5652, 1993.
- [33] C. Lee, W. Yang, and R. G. Parr, “Development of the Colle-Salvetti correlation-energy formula into a functional of the electron density,” *Physical Review B: Condensed Matter and Materials Physics*, vol. 37, no. 2, pp. 785–789, 1988.
- [34] A. Schäfer, C. Huber, and R. Ahlrichs, “Fully optimized contracted Gaussian basis sets of triple zeta valence quality for atoms Li to Kr,” *The Journal of Chemical Physics*, vol. 100, no. 8, pp. 5829–5835, 1994.
- [35] P. Pulay, “Convergence acceleration of iterative sequences. the case of scf iteration,” *Chemical Physics Letters*, vol. 73, no. 2, pp. 393–398, 1980.
- [36] P. Pulay, “Improved SCF convergence acceleration,” *Journal of Computational Chemistry*, vol. 3, no. 4, pp. 556–560, 1982.
- [37] A. D. Becke and K. E. Edgecombe, “A simple measure of electron localization in atomic and molecular systems,” *The Journal of Chemical Physics*, vol. 92, no. 9, pp. 5397–5403, 1990.
- [38] G. Pacchioni and G. Ieranò, “Computed optical absorption and photoluminescence spectra of neutral oxygen vacancies in  $\alpha$ -quartz,” *Physical Review Letters*, vol. 79, no. 4, pp. 753–756, 1997.
- [39] T. Uchino, M. Takahashi, and T. Yoko, “Mechanism of interconversion among radiation-induced defects in amorphous silicon dioxide,” *Physical Review Letters*, vol. 86, no. 9, pp. 1777–1780, 2001.



Hindawi

Submit your manuscripts at  
[www.hindawi.com](http://www.hindawi.com)

